ARTICLE OPEN

Check for updates

Suprachiasmatic nucleus dysfunction induces anxiety- and depression-like behaviors via activating the BDNF-TrkB pathway of the striatum

Xiaotao Liang[1,2], Yuewen Ding[1,2], Xiaoyu Zhu[1], Jing Qiu[1], Xiaoqin Shen[1], Yifan Xiong[1], Jieli Zhou[1], Xiaoshan Liang[2]✉ and Wei Xie[1,3]✉

The circadian rhythm system consists of a master clock located in the suprachiasmatic nucleus (SCN) of the hypothalamus and peripheral clocks dispersed throughout other brain areas (including striatum, Str) as well as various tissues and organs. Circadian rhythm disturbance is a major risk factor and common comorbidity for mood disorders, especially anxiety and depression. Bmal1 is one of the fundamental clock protein genes that is required to maintain circadian rhythm. Recent research has revealed a link between suprachiasmatic nucleus dysfunction and anxiety and depression, but the underlying mechanisms remain to be fully elucidated. This study aimed to investigate how circadian rhythm disturbance may lead to anxiety- and depression-like behaviors. Through behavioral tests, virus tracing, molecular biology and other techniques, we found neural connection from the suprachiasmatic nucleus to the striatum. SCN lesions and Bmal1$^{flox/flox}$ + pAAV-hSyn-Cre-GFP (conditional knockout, cKO) mice exhibited disruptions in core body temperature rhythm, as well as anxiety- and depression-like behaviors. Importantly, these mice displayed altered expression patterns of clock protein genes and an upregulation of the Brain-Derived Neurotrophic Factor (BDNF) - Tyrosine Kinase receptor B (TrkB) signaling pathway within the striatum. Microinjection of the TrkB inhibitor ANA-12 can effectively reverse anxiety- and depression-like behaviors. These findings indicate that suprachiasmatic nucleus dysfunction may contribute to the pathogenesis of anxiety and depression through upregulation of the BDNF-TrkB pathway in the striatum, potentially mediated by neural projections from the SCN. Bmal1 gene within SCN may represent a novel therapeutic target for mood disorders.

Translational Psychiatry (2025)15:92 ; https://doi.org/10.1038/s41398-025-03313-7

INTRODUCTION

The circadian system regulates physiological, cellular and behavioral rhythms that are about 24 h in duration. It is regulated by interlocking transcription-translation feedback loops (TTFL) controlled by clock genes, including transcriptional activators like Bmal1 and Clock, and repressors like Cry and Per. This rhythm consists of the master clock located in the suprachiasmatic nucleus (SCN) of the hypothalamus, as well as peripheral clocks in various brain regions and other organs [1]. Accumulating evidence indicate that circadian disturbances might contribute to occurrence and progression of mood disorders, including anxiety and depression [2–5].

Anxiety and depression are frequently accompanied by symptoms associated with circadian rhythm disorders like difficulty falling asleep and early awakening, and can be attributed to abnormalities in circadian genes [6]. Depression episodes manifest a cyclical pattern, with severe morning symptoms which subsides in the evening, accompanied by decreased circadian gene amplitudes [7–9]. Circadian disruption heightens the risk of anxiety and depression by 25–40% and is a predictor of recurrence [10–12]. While numerous studies strongly suggest that deleting certain circadian rhythm genes makes individuals more susceptible to anxiety and depression [13–15], the exact reason for this link remains unclear. This is especially true regarding the specific role of the SCN, the brain region responsible for regulating the body's internal clock.

The efferent fibers of SCN mainly project to the ventromedial preoptic area (VMPO) and ventrolateral preoptic area (VLPO), thalamus, and limbic system, thus connecting with important brain areas related to mental emotions [16]. The striatum (Str), a brain region involved in emotions, memory, and thinking, acts as an internal clock. This is particularly true for the ventral part of the striatum, which includes the mesolimbic pathway of ventral tegmental area (VTA) and the nucleus accumbens (NAc). These areas show a strong daily rhythm in their activity [17–20]. In the striatum, the expression levels of BDNF-TrkB pathway exhibit a circadian rhythm, and contributes to the pathogenesis of anxiety and depression [21–24]. Thus, we hypothesized that dysfunction in the suprachiasmatic nucleus, which affects the circadian rhythm, can induce anxiety- and depression-like behaviors via the BDNF-TrkB pathway in the striatum.

This study aimed to investigate whether suprachiasmatic nucleus dysfunction induced anxiety- and depression-like behaviors. First, we stereotaxically injected AAV1-hSyn-eGFP into the SCN to observe the

[1]School of Traditional Chinese Medicine, Southern Medical University, Guangzhou 510515, P.R. China. [2]Department of Traditional Chinese Medicine, Nanfang Hospital, Southern Medical University, Guangzhou 510515, P.R. China. [3]Guangdong Basic Research Center of Excellence for Integrated Traditional and Western Medicine for Qingzhi Diseases, Guangzhou 510515, P.R. China. ✉email: liangxiaoshan@smu.edu.cn; xieweizn@smu.edu.cn

Received: 19 June 2024 Revised: 18 February 2025 Accepted: 11 March 2025
Published online: 21 March 2025

neural projections. Moreover, we performed bilateral SCN lesions in C57BL/6 J mice and injected AAV2/5-hSyn-Cre-GFP adeno-associated virus into the SCN of Bmal1$^{flox/flox}$ mice to construct circadian rhythm disorder model, and evaluated the anxiety- and depression-like behaviors of them using temperature monitoring and behavioral testing. Finally, we explored the effects of the clock protein genes and BDNF-TrkB pathway using molecular biology.

MATERIALS AND METHODS

Animals

All animal experiments were approved by the Laboratory Animal Research Committee of Southern Medical University (permit number: L2021009). Male 8-week-old C57BL/6 J mice (Experimental Animal Center of Southern Medical University, Guangzhou, China) and Bmal1$^{flox/flox}$ mice (described below) were used. All mice were housed under controlled temperature (25 °C ± 1 °C) and humidity (50% ± 5%) with ad libitum access to food and water. Furthermore, the mice were kept at a 12-h light/dark (LD) cycle, with the light phase commencing at 7:00 AM (Zeitgeber Time 0, ZT0) and stopping at 7:00 PM (ZT12) for one week before experiments. The animal experiments followed the ARRIVE guidelines and National Research Council's Guide for the Care and Use of Laboratory Animals. Also, the animal experiments were approved by the Laboratory Animal Ethics Committee of Southern Medical University (Guangzhou, China). Animal experiments were carried out in a blinded manner; the experimenters were unaware of the group assignment and treatment conditions.

SCN lesions

Bilateral SCN lesions were created in C57BL/6 J mice under 3% isoflurane-induced anesthesia via stereotactic procedure. Briefly, a small cranial aperture was carefully created using a dental drill bur (0.25 mm posterior to bregma and 0.2 mm lateral from the midline). A platinum-iridium alloy electrode (diameter; 0.15 mm), sheathed entirely in polyimide except for a 0.2 mm exposed tip, was bilaterally inserted into the SCN (depth; 6.10 mm) from the skull surface. A direct electrical current (0.6 mA) was applied for 60 s with a Ugo Basile lesion maker before withdrawal from the brain. A similar procedure was also conducted on the sham group, except for the electrical current application.

SCN- specific Bmal1- knockout mice (cKO)

Bmal1$^{+/-}$ mice were acquired from Shanghai Model Organisms Center, Inc. (Shanghai, China). Homozygous Bmal1$^{flox/flox}$ mice were generated by mating with Bmal1$^{+/-}$ mice and genetically identified via PCR using gene-specific primers (Fig. S1). Subsequently, the Bmal1$^{flox/flox}$ mice were randomly assigned to two groups and stereotactically injected with AAV2/5-hSyn-Cre-GFP or AAV2/5-hSyn-GFP (titer: 1.6×10^{12} VG/ml in saline, generated by Shanghai Jikai Gene Medicine Technology Co., Ltd., Shanghai, China). The hSyn promoter, which drives the expression of Cre recombinase, is tightly integrated with target neurons via the adeno-associated virus AAV2/5. Bmal1$^{flox/flox}$ + pAAV-hSyn-Cre-GFP mice were constructed by injecting AAV2/5-hSyn-Cre-GFP adeno-associated virus into the SCN of Bmal1$^{flox/flox}$ mice. Four weeks after the microinjection, the mice were used in experiments.

Trans-synaptic tracing

AAV1-hSyn-eGFP was utilized for anterograde trans-synaptic tracing to investigate the neural circuit between the SCN and the striatum (Str). Specifically, 0.3 μL of AAV1-hSyn-eGFP, with anterograde trans-synaptic properties, was stereotactically injected into the SCN (coordinates: AP: −0.2 mm, ML: ±0.25 mm, DV: −6.10 mm from bregma) to label SCN projection neurons. Frozen brain sections were collected 3–4 weeks post-injection to analyze downstream brain regions. These sections were subsequently subjected to immunofluorescence labeling with c-Fos and DAPI for histological and fluorescence distribution analyses.

Additionally, the retrograde tracer cholera toxin B (CTB) was injected into the striatum (coordinates: AP: 0.5 mm; ML: ±2.0 mm; DV: −3.5 mm from bregma) (Fig. S2a) to complement the investigation. Frozen brain sections were collected 3–4 weeks post-injection to analyze upstream brain regions.

Drug administration

After anesthetizing the mice, their heads were secured in a stereotaxic frame (RWD Life Science, Shenzhen, China). Two holes were drilled into the skull at stereotaxic coordinates (AP: 0.5 mm; ML: ±2.0 mm from bregma). A single cannula (Cannula-Single/O.D. 0.48 mm, 26 G/M3.5; Reward, Shenzhen, China) was carefully clamped and lowered bilaterally through the holes at a 9° angle until the tips reached the striatum (AP: 0.5 mm; ML: ±2.0 mm; DV: −3.5 mm from bregma). ANA-12, a selective tropomyosin receptor kinase B (TrkB) inhibitor, was bilaterally infused into the striatum (1 μg/μL, 0.5 μL per side). The injection was conducted 2 h prior to each behavioral experiment at stereotaxic coordinates. The dosage was chosen based on preliminary data and previous studies, which indicated no adverse effects on mouse behavior [25, 26]. A total volume of 0.5 μL was infused into each side over 15 min.

Dynamic core body temperature monitoring

First, the dorsal fascia was surgically separated, followed by wrapping of the button-type temperature recorder (iButton) into the longitudinal incision cut under isoflurane-induced anesthesia. The incision was then sutured using absorbable sutures and disinfected with alcohol. The iButton recording data at 15-min intervals for a minimum of 10 days was retrieved, then the temperature data was imported into ENLOG analysis to create an activity diagram. The temperature deviation from the baseline (35 °C) was considered as the statistical dataset and input into the formula below: (Y=Amplitude × cos [(X / Wavelength) + PhaseShift] +Baseline). Finally, Graphpad Prism software was used to construct a 24-h circadian rhythm chart.

Behavioral procedures

The mice underwent behavioral laboratory tests for 30 min before each experiment. The behavioral experiments were performed between 9:00 a.m. and 6:00 p.m. Behaviors were recorded, stored, and analyzed using an automated behavioral tracking system (Smart 3.0.06, Panlab Harvard Apparatus) equipped with infrared lighting-sensitive CCD cameras.

Open field test (OFT)

The mice were individually placed in the center of an open-field apparatus (50 cm × 50 cm), which was illuminated with one yellow lights (40 W) fluorescent lamps located 100 cm above the ground. The mice were placed in the center square (20 cm × 20 cm) at the beginning of the experiment and allowed to freely explore for 6 min. The total distance covered in last 5 min, distance in center, time spent in center and entries in center were monitored via video-tracking system. The maze was washed with 75% ethanol between trials to avoid odor cues.

Elevated plus maze test (EPM)

The mice were put in a standard elevated plus maze with two open arms and closed arms perpendicular to each other (30 cm × 5 cm) and a connecting central platform (5 cm × 5 cm). The maze was elevated 50 cm above the floor, where the closed arm was surrounded by an opaque partition (height; 15 cm). Each mouse was placed in the center of the maze facing one of the open arms and observed for 5 min. The residence time and movement process of the open and closed arms were recorded.

Sucrose preference test (SPT)

Anhedonia is one of the main symptoms of depression. Anhedonia can be assessed using the sucrose preference test (SPT), a reward-based assessment. In this study, the mice were individually given free access to two bottles in the cage, one containing water and the other 1% sucrose solution, as previously described. The preference for the sweet solution, calculated as a percentage of the sucrose intake over the total fluid intake and averaged over the testing period, was measured daily. Notably, the mice were acclimated to having two drinking bottles in the cages for at least two days before the tests. The bottles were counterbalanced across the left and the right sides of the cage and positions were alternated every 12 h. Sucrose preference was calculated as follows: Sucrose preference = V (sucrose solution)/ [V (sucrose solution) +V(water)] x 100%.

Tail suspension test (TST)

The mice's tail (1 cm from the tip) was fastened on a hook about 20 cm off the floor, allowing them to hang freely without touching any surfaces with their feet or tail. Once the mice are correctly tied, their activity is observed and recorded for a period of six minutes. Shanghai Xinsoft Behavioral Software is used to correctly monitor and log each mouse's immobility length across the 6-min test period [27].

Forced swimming test (FST)
The mice were placed in a plexiglass cylinder (diameter: 12 cm, height: 25 cm) containing water (height, 15 cm). The water was replaced after every test, and its temperature was maintained at 24 ± 1 °C. The mice underwent pre-swimming habituation training for 5 min a day before the test. The mice were made to swim for 6 min straight on the test day, Immobility was quantified in the last 5 min of the test using the video-tracking system after a one-minute warm-up swim.

Nissl staining
SCN tissue samples were fixed in 4% paraformaldehyde at room temperature overnight and cut into 5 μm sections. The sections were soaked in Nissl staining solution toluidine blue after treatment with a series of increasing concentrations of 75–100% alcohol to remove moisture. The tissue samples were destained in decreasing concentrations of alcohol and soaked in sorbitol. Finally, the tissue samples were placed on a glass slide and covered with mounting medium for visualization under a microscope.

Quantitative real-time polymerase chain reaction (qRT-PCR)
As previously reported [28], mice were euthanized at 6-h intervals over a 24-h period at ZT0, ZT6, ZT12, ZT18, and ZT24 for each group. Euthanasia was performed within 20 min of each designated ZT. For ZT0, ZT18, and ZT24, the procedure was conducted under dim red light to minimize light. Total RNA was extracted from the SCN and striatum using the TRIzol reagent following the manufacturer's instructions [29]. The concentration and purity of mRNA were assessed using a DS-C 260/280 and 260/230 ratio spectrophotometer. Each sample RNA (1 μg) was reverse transcribed into cDNA using the PrimeScriptTM RT Kit. RT-qPCR was performed on a LightCycler 96 instrument using SYBR® Premix Ex Taq™. The polymerase chain reaction was run as follows: 40 cycles were performed at 95 °C for 5 s, 60 °C for 30 s, and 72 °C for 30 s after a first cycle at 95 °C for 30 s with an initial DNA denaturation step. CT (threshold cycle) readings were predefined. The relative expression of target gene mRNA was determined using the 2-ΔΔCT method. The average value of glycerol-3-phosphate dehydrogenase (GAPDH) was used as the internal reference for normalization.

Western blot analysis
Striatal tissues were collected at a designated time point (ZT6) and processed in RIPA buffer supplemented with protease and phosphatase inhibitors to preserve protein integrity. The extracted proteins were separated using SDS-PAGE, transferred to a PVDF and blocked with 5% BCA blocking solution. The membranes were subsequently incubated with primary antibodies at 4 °C overnight. The resulting data was analyzed via immunoblotting after incubation with HRP-conjugated secondary antibodies. Antibodies used in western blotting included: TrkB, BDNF, CREB, p-CREB, ERK1/2, p-ERK1/2.

Immunofluorescence staining
First, the tissue sections were fixed with 4% formaldehyde at room temperature for 15 min, washed with phosphate-buffered saline (PBS), permeabilized with 0.1% Triton X-100 for 10 min and incubated with 2.5% goat serum to block non-specific binding. The sections were incubated with anti-c-Fos antibody at 4 °C overnight. The sections were washed with PBS, then incubated with Fluorescent-labeled Alexa Fluor 594-conjugated anti-mouse IgG at room temperature for 1 h. The sections were counter-stained with DAPI for visualization using an inverted fluorescent microscope.

GEO data sets analysis
Gene expression data (GSE76826 profiling data) were obtained in raw signal format from the Gene Expression Omnibus (http://www.ncbi.nlm.nih.gov/geo). Subsequent steps, including interpretation, normalization, and log2 scaling, were performed using the online analysis platform provided by GCBI (https://www.gcbi.com.cn). Differentially expressed gene sets between normal and individuals with depression within the GSE76826 dataset were identified using the online tools available on the GCBI platform (Fig. S3).

Sample size determination and statistical considerations
The sample size for this study was determined based on insights from previous research and preliminary experiments to ensure sufficient power for detecting the pre-specified effect size [28]. In the preliminary experiments, the efficiency of electrofusion and virus injection was evaluated using Nissl staining, temperature monitoring, and q-PCR, yielding a success rate of 90%. To minimize the number of animals used while maintaining statistical robustness, mice that experienced excessive bleeding or mortality due to electrofusion or virus injection were excluded. Ultimately, each group comprised 15 animals.

Statistical analysis
The analysis of experimental data in this study was conducted in a double-blind manner to ensure unbiased results. All statistical analyses were performed using GraphPad Prism 8. The data were expressed as the means ± SEM unless otherwise specified. The experiments were performed in triplicate. The Kruskal–Wallis test, unpaired t-test, and one-way analysis of variance (ANOVA) with post hoc multiple comparison tests were performed as indicated in the figure legends. The circadian cosinor method, implemented using Cosinor software, was applied to determine the rhythmic amplitude of daily temperature and mRNA oscillations. In Prism, a cosine transformation with a 24-h circadian cycle was used to analyze the time-variable data for daily temperature and mRNA oscillations. The analysis was performed using a nonlinear regression equation: $y = \text{baseline} + \text{amplitude} \times \cos((\text{frequency} \times x) + \text{phase shift}))$. This approach allows for precise quantification of rhythmic patterns in the data. $p < 0.05$ was considered statistically significant ($*p < 0.05$, $**p < 0.01$).

RESULTS
Activation of neural connection from the SCN to the striatum mediated by SCN lesions
Anterograde tracers are widely used in neural circuit analysis. To explore whether the SCN projects to the striatum (Str), AAV1-hSyn-eGFP, which expresses GFP with a nuclear localization signal, was employed. AAV1 has been demonstrated to mediate anterograde transsynaptic tagging, allowing for neuronal circuit probing. Connection from the SCN to the Str would therefore lead to the expression of nuclear GFP in Str neurons.

In this study, we injected the anterograde tracer virus AAV1-hSyn-eGFP into the SCN (Fig. 1a). Anterograde tracing results showed that eGFP exhibited green fluorescence in the SCN, confirming effective viral delivery (Fig. 1b). Between 3 to 4 weeks following injection, neuron in the striatum also expressed green fluorescence, indicating neural connection from the SCN to the striatum (Fig. 1c).

Additionally, we injected the retrograde tracer cholera toxin B (CTB) into the striatum (Fig. S2a). Successful deposition of CTB was confirmed by the presence of red fluorescence in striatal neurons (Fig. S2b). Notably, after 3–4 weeks, red fluorescence was also observed in neurons within the SCN, further supporting the existence of reciprocal neural circuits between the SCN and the striatum (Fig. S2c).

Then, we performed bilateral SCN lesions on C57BL/6 J mice using stereotactic techniques and direct electrical current (1.0 mA for 60 s). Following SCN lesions, we observed an increase in c-Fos expression and fluorescence intensity in the striatum compared to the sham group (Fig. 1d, e). However, there was no statistically significant difference in the fluorescence intensity of eGFP between the two groups (Fig. 1f). This indicates that lesions to the SCN can activate neural connection from the SCN to the striatum.

SCN lesions and conditional knockout of Bmal1 induced circadian rhythm disorder
To evaluate the effects of suprachiasmatic nucleus dysfunction on circadian rhythm disorders, we performed bilateral SCN lesions and administered the AAV2/5-hSyn-Cre-GFP virus for a conditional Bmal1 knockout (cKO). An iButton device was implanted in mouse to continuously monitor body temperature (Fig. 2a). Nissl staining demonstrated substantial structural damage to SCN neurons in the lesion group compared to the sham group (Fig. 2b). Immunofluorescence confirmed successful Bmal1 knockout, indicated by significantly diminished Bmal1 fluorescence in the SCN (Fig. 2l).

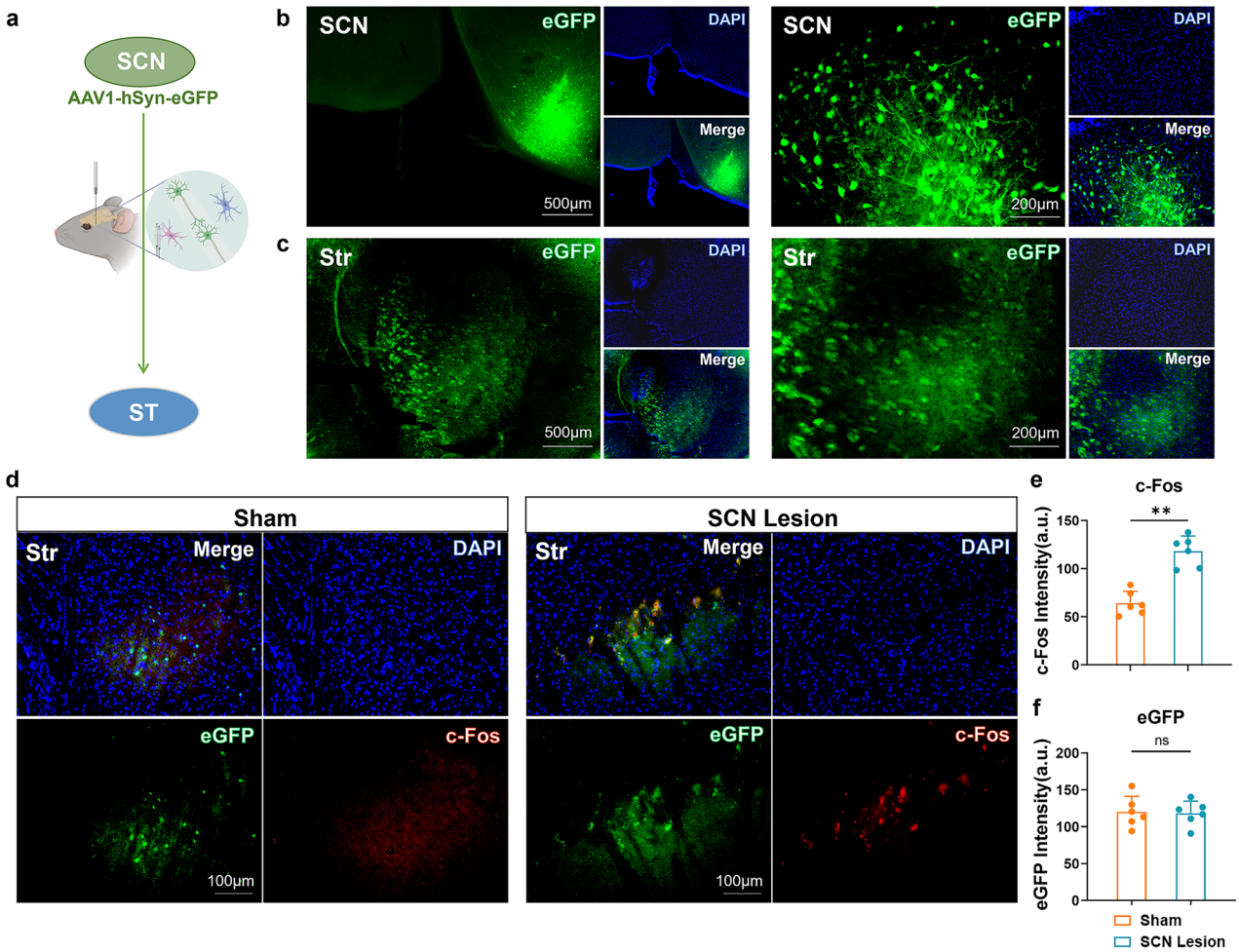

Fig. 1 Bilateral SCN lesions activated neural circuit connection between the SCN and striatum. a Neural tracer map. **b, c** Anterograde tracing from the SCN to the Striatum. (eGFP, green; DAPI, blue). Scale bars = 500 and 200 μm. **d** Representative images of Immunofluorescence staining in the striatum of Sham and SCN Lesion groups. (eGFP, green; c-Fos, red; DAPI, blue). **e** Analysis of c-Fos Intensity. n = 6, per group. **f** Analysis of eGFP Intensity. n = 6, per group. Data are expressed as mean ± SEM, ANOVA, $*p < 0.05$, $**p < 0.01$, by two-tailed unpaired Student's t test. eGFP, AAV1-hSyn-eGFP.

Temperature monitoring under constant environmental conditions revealed that the sham group displayed a pronounced peak in body temperature during the middle of the subjective night. Conversely, the SCN lesion group exhibited erratic temperature fluctuations with dual peaks during the subjective day and night, suggesting altered temperature rhythms (Fig. 2c, d). Similarly, the conditional knockout (cKO) group showed a disrupted circadian temperature pattern with two less pronounced peaks and significantly reduced temperature oscillation amplitude, unlike the control group which maintained a normal circadian rhythm with a typical nocturnal temperature peak (Fig. 2m, n). These findings collectively suggest that both SCN lesions and the conditional knockout of Bmal1 in SCN neurons contribute to SCN dysfunction, leading to significant disruptions in circadian rhythms.

SCN lesions and conditional knockout of Bmal1 induced anxiety- and depression- like behaviors

To evaluate the impact of SCN lesions on anxiety and depression, behavioral assessments were conducted 10 days post-lesion (Fig. 2a). In the Open Field Test (OFT), compared with sham mice, SCN lesion mice spent less time and made fewer entries in the center, although their overall activity levels did not differ (Fig. 2e, f). In the Elevated Plus Maze (EPM), compared to sham mice, SCN lesion mice spent less time and made fewer entries in the open arms, while spending more time in the closed arms (Fig. 2g, h). Also, compared with sham mice, SCN lesion mice demonstrated a less sucrose preference rate in the Sucrose Preference Test (SPT) (Fig. 2i), a longer immobility time in the Tail Suspension Test (TST) (Fig. 2j) and Forced Swim Test (FST) (Fig. 2k).

Behavioral tests were initiated 3 weeks after the virus injection to evaluate the effect of the Bmal1 knockout on anxiety- and depression-like behaviors. In the OFT, compared with control mice, cKO mice spent less time and made fewer entries in the center, although their overall activity levels did not differ (Fig. 2o, p). In the EPM, compared to control mice, cKO mice spent less time and made fewer entries in the open arms, while spending more time in the closed arms (Fig. 2q, r). These findings suggested anxiety-like behaviors in cKO mice. Also, compared with control mice, cKO mice demonstrated a less sucrose preference rate in the SPT (Fig. 2s), a longer immobility time in the TST (Fig. 2t) and FST (Fig. 2u).

Overall, the above results indicate that dysfunction in the suprachiasmatic nucleus, whether induced by physical lesions or genetic manipulation via Bmal1 knockout, leads to significant anxiety- and depression-like behaviors.

SCN lesions and conditional knockout of Bmal1 altered the oscillation amplitude of circadian genes in the striatum

The expression levels of circadian genes in the striatum were assessed at different times of the day (ZT0, ZT6, ZT12, ZT18, ZT24) using RT-qPCR to evaluate the effect of bilateral SCN lesions and conditional knockout of Bmal1. Compared with sham group, the

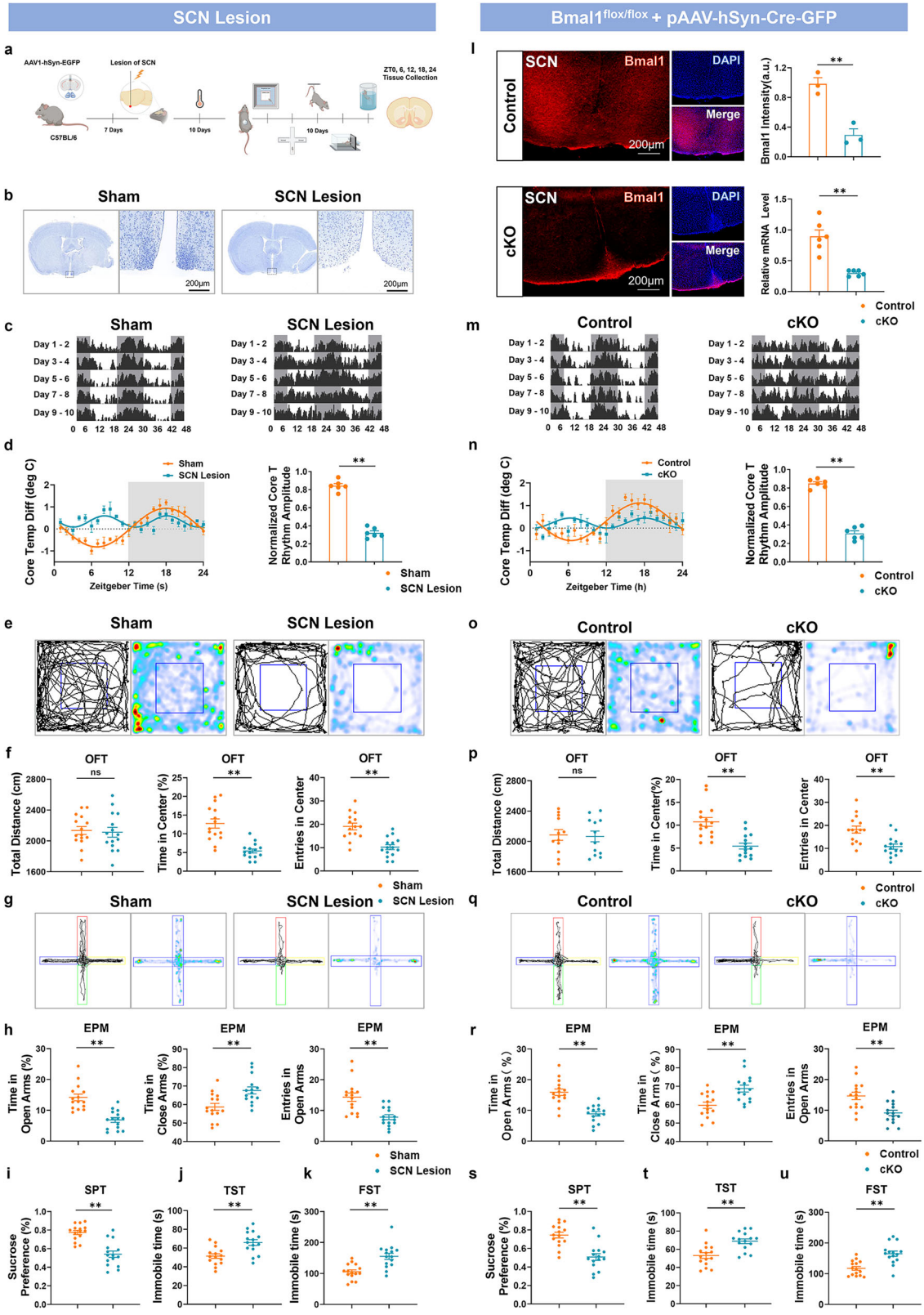

oscillation amplitude of Bmal1, Clock, Cry1 and Cry2 was significantly decreased in SCN lesion group (Fig. 3a–d), while that of Per1 and Per2 significantly increased (Fig. 3e, f). Furthermore, the total mRNA levels of Bmal1, Clock, Per1, and Per2 genes in the striatum were significantly increased in SCN lesion group (Fig. 3a, b, e, f), while the total mRNA expression levels of Cry1 and Cry2 significantly reduced in SCN lesion group (Fig. 3c, d).

Compared with control group, cKO group demonstrated a decrease oscillation amplitude of Bmal1 and Clock in the striatum (Fig. 3g, h), while this of Per1 and Per2 significantly increased (Fig.

Fig. 2 Bilateral SCN lesions and Conditional knockout of Bmal1 disrupted core body temperature and induced anxiety- like and depression- like behaviors in mice. a Experimental design. **b** Representative images of Nissl staining in the SCN of Sham and SCN Lesion groups. Scale bar = 200 μm. n = 3 per group. **c** Continuous monitoring of core body temperature in the Sham and SCN Lesion groups over a 10-Day Period. **d** Cosine curve graph of core body temperature and statistical analysis of core body temperature oscillation amplitude. n = 6 per group. **e** Trajectory map of Sham and SCN Lesion groups in the OFT. **f** The behavioral test of the Sham and SCN Lesion groups. Total distance, center time percentage, and entries into center in the OFT (n = 15, respectively). **g** Trajectory map of Sham and SCN Lesion groups in the EPM. **h** Open arms time percentage, entries into open arms, and close arms time percentage in the EPM (n = 15, respectively). **i** Sucrose preference percentage in the SPT (n = 15, respectively). **j** Immobility time in the TST (n = 15, respectively). **k** Immobility time in the FST (n = 15, respectively). **l** Representative images of Bmal1 expression and intensity in the SCN of Control and cKO mice (Bmal1, red; DAPI, blue, scale bars = 200 μm. n = 3, per group) and SCN relative Bmal1 mRNA level of Control and cKO groups (n = 6, per group). **m** Continuous monitoring of core body temperature in the Control and cKO groups over a 10-Day Period. **n** Cosine curve graph of core body temperature and statistical analysis of core body temperature oscillation amplitude. n = 6 per group. **o** Trajectory map of Control and cKO groups in the OFT. **p** The behavioral test of the Control and cKO groups. Total distance, center time percentage, and entries into center in the OFT (n = 15, respectively). **q** Trajectory map of Control and cKO groups in the EPM. **r** Open arms time percentage, entries into open arms, and close arms time percentage in the EPM (n = 15, respectively). **s** Sucrose preference percentage in the SPT (n = 15, respectively). **t** Immobility time in the TST (n = 15, respectively). **u** Immobility time in the FST (n = 15, respectively). Data are expressed as mean ± SEM, ANOVA, $*p < 0.05$, $**p < 0.01$, by two-tailed unpaired Student's t test. OFT, open field test; EPM, elevated plus maze test; SPT, sucrose preference test; TST, tail suspension test; FST, forced swim test.

3k, l). Furthermore, compared with control group, cKO group demonstrated an increase total mRNA level of Bmal1, Clock, Per1, and Per2 in the striatum (Fig. 3g, h, k, l). However, the expression level of Cry1, oscillation amplitude of Cry1 and Cry2 did not significantly change in the cKO group (Fig. 3i, j).

Taken together, these findings demonstrate that SCN lesions and Bmal1 knockout significantly disrupt the oscillation amplitude and total mRNA level of circadian genes in the striatum, underlining the profound influence of SCN integrity on circadian regulation within this brain region.

SCN lesions and conditional knockout of Bmal1 upregulated the BDNF-TrkB pathway in the striatum

BDNF plays an important role in the pathogenesis of anxiety and depression [30]. In this study, we used qRT-PCR and Western blot to assess circadian variations of BDNF in the striatum. In the sham group, BDNF mRNA levels exhibited a rhythmic pattern, increasing at night and decreasing during the day. In contrast, in the SCN lesion group, the mRNA levels of BDNF, especially during the daytime (ZT6), were significantly elevated. Additionally, the oscillation amplitude of BDNF also showed a marked increase in this group (Fig. 4a–c). Given the pivotal role of the BDNF-TrkB pathway in regulating the mental illness [31], we further evaluated the expression levels of key proteins in this pathway, including BDNF, TrkB, CREB, ERK, p-CREB, and p-ERK1/2. Our results revealed that SCN lesions lead to increased expression levels of BDNF, TrkB, p-CREB, and p-ERK1/2 (Fig. 4d–h), while the total protein level of CREB and ERK1/2 remained unchanged.

Similarly, in the cKO group, we observed a significant increase in the total mRNA levels and oscillation amplitude of BDNF in the striatum compared to the control group (Fig. 4i–k). Protein expression analysis further demonstrated that the cKO group had elevated levels of BDNF, TrkB, p-CREB, and p-ERK1/2 in the striatum (Fig. 4l–p), whereas the total protein level of CREB and ERK1/2 were unchanged.

Taken together, these results collectively indicate that disturbances in the SCN, whether caused by SCN lesions or Bmal1 knockout, lead to upregulation of the BDNF-TrkB pathway in the striatum. This suggests that the Bmal1 gene plays a crucial role in maintaining normal SCN function and regulating the BDNF-TrkB pathway in the striatum, potentially influencing the pathophysiology of anxiety and depression.

TrkB receptor antagonist ANA-12 reversed anxiety- and depression-like behaviors in SCN Lesion and cKO mice

The TrkB receptor is the primary receptor for BDNF, playing a crucial role in neuronal survival, development, and plasticity. ANA-12, a potent and selective TrkB antagonist, binds directly to TrkB and inhibits its downstream signaling pathways [32].

We investigated the effects of local ANA-12 infusion (1 μg/μL, 0.5 μL per side, administered 2 h before testing) on anxiety- and depression-like behaviors (Fig. 5a, i). In the OFT, SCN lesion + ANA-12 mice exhibited significant anti-anxiety and antidepressant effects compared to SCN lesion mice, including increased time spent in the center and a higher number of center entries (Fig. 5b, c). In the EPM, SCN lesion + ANA-12 mice demonstrated an increased time spent in open arms, a higher number of open arms entries and a decreased time spent in close arms (Fig. 5d, e). Furthermore, SCN lesion + ANA-12 mice demonstrated a higher sucrose preference rate in the SPT (Fig. 5f), a shorter immobility time in the TST (Fig. 5g) and FST (Fig. 5h).

Similarly, in conditional knockout (cKO) mice, ANA-12 infusion yielded comparable anti-anxiety and antidepressant effects. cKO + ANA-12 mice spent more time in the center and made more center entries in the OFT (Fig. 5j, k). In the EPM, these mice exhibited increased time in the open arms, more open-arm entries, and reduced time in the closed arms (Fig. 5l, m). They also displayed higher sucrose preference in the SPT (Fig. 5n) and reduced immobility times in the TST (Fig. 5o) and FST (Fig. 5p). These results indicate that dysfunction of the suprachiasmatic nucleus (SCN) may promote anxiety- and depression-like behaviors through activation of the BDNF-TrkB signaling pathway. The observed therapeutic effects of ANA-12 underscore its potential for mitigating these behaviors by inhibiting TrkB signaling.

TrkB receptor antagonist ANA-12 downregulated BDNF-TrkB signaling in the striatum

We utilized q-PCR to examine the circadian rhythm variations in BDNF expression over a 24-h cycle (ZT0 to ZT24). To further evaluate the effects of local ANA-12 infusion on BDNF-TrkB signaling in the striatum, striatal tissue samples were collected at ZT6 for Western blot analysis.

The results revealed that ANA-12 infusion significantly reduced both the mRNA levels and the circadian rhythm amplitude of BDNF in the striatum, along with suppressing BDNF-TrkB signaling. In the SCN lesion + ANA-12 group, the mRNA levels and circadian rhythm amplitude of BDNF were markedly lower than those in the SCN lesion group (Fig. 6a–c). Similarly, the protein expression levels of TrkB, BDNF, p-ERK/ERK, and p-CREB/CREB were significantly decreased in comparison to the SCN lesion group (Fig. 6d–h). In contrast, no significant differences in these protein expression levels were observed between the sham and sham + ANA-12 groups (Fig. 6d–h).

A similar pattern was observed in the cKO + ANA-12 group, where the mRNA levels and circadian rhythm amplitude of BDNF were significantly reduced compared to the cKO group (Fig. 6i–k). Moreover, the expression levels of TrkB, BDNF, p-ERK/ERK, and p-CREB/CREB were significantly lower than those in the cKO group

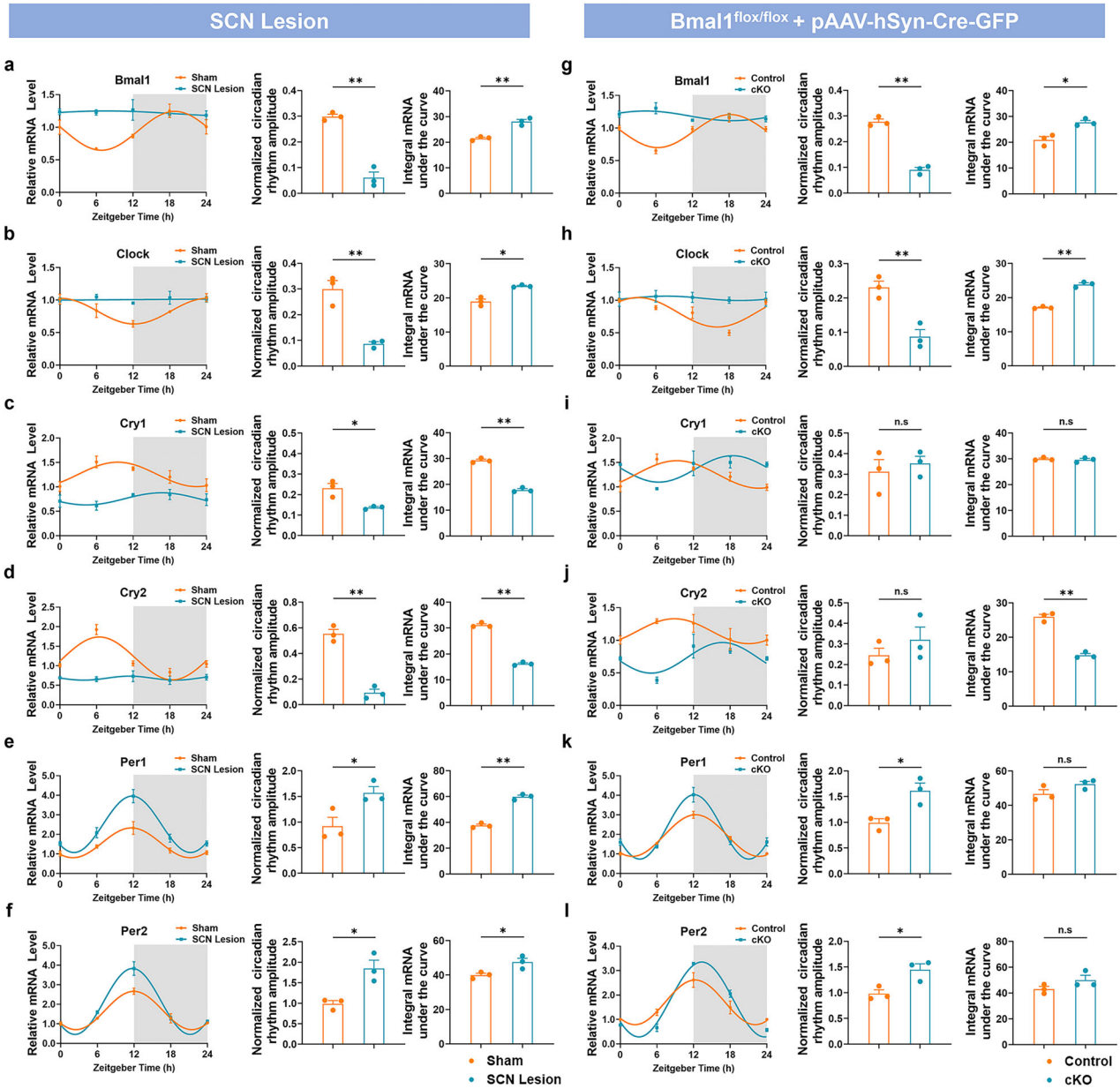

Fig. 3 Bilateral SCN lesions and Conditional knockout of Bmal1 disrupted striatal total mRNA levels and oscillation amplitudes of circadian genes. a Cosine curve graph of striatal relative mRNA level, normalized circadian rhythm amplitude and integral mRNA under the curve of Bmal1 in Sham and SCN Lesion groups; **b** Clock; **c** Cry1; **d** Cry2; **e** Per1; **f** Per2. n = 3. **g** Cosine curve graph of striatal relative mRNA level, normalized circadian rhythm amplitude and integral mRNA under the curve of Bmal1 in Control and cKO groups; **h** Clock; **i** Cry1; **j** Cry2; **k** Per1; **l** Per2. n = 3. Data are expressed as mean ± SEM, ANOVA, $*p < 0.05$, $**p < 0.01$, by two-tailed unpaired Student's t test. Bmal1, ARNT-like rotein-1; Clock, Clock circadian regulator gene; Cry1, Cryptochrome circadian clock 1; Cry2, Cryptochrome circadian clock 2; Per1, Period protein gene-1; Per2, Period protein gene-2.

(Fig. 6l–p). However, no significant differences were detected between the control and control + ANA-12 groups (Fig. 6l–p).

These findings indicate that local ANA-12 infusion effectively mitigates anxiety- and depression-like behaviors by downregulating BDNF-TrkB signaling in the striatum of mice with circadian rhythm disruptions.

DISCUSSION

Circadian rhythms significantly influence human mood fluctuations, as established in prior studies [5, 33]. This research elucidates how dysfunctions in the suprachiasmatic nucleus (SCN), the master regulator of circadian rhythms, impact mood disorders such as anxiety and depression. Our findings highlight the critical role of the BDNF-TrkB pathway in the striatum, influenced by SCN dysfunction, in the manifestation of these disorders. In this study, we developed a mouse model with SCN lesions and observed disturbances in the 24-h circadian regulation of core body temperature, along with behaviors indicative of anxiety and depression. These alterations were accompanied by activation of neural connection from the SCN to the striatum, disruption in circadian clock genes expression, and upregulation of BDNF-TrkB pathway in the striatum. Moreover, we obtained similar results in a mouse model with conditional knockout of the Bmal1 gene in the SCN (cKO). These demonstrate the potential mechanism by which SCN dysfunction may contribute to occurrence of behaviors of anxiety and depression.

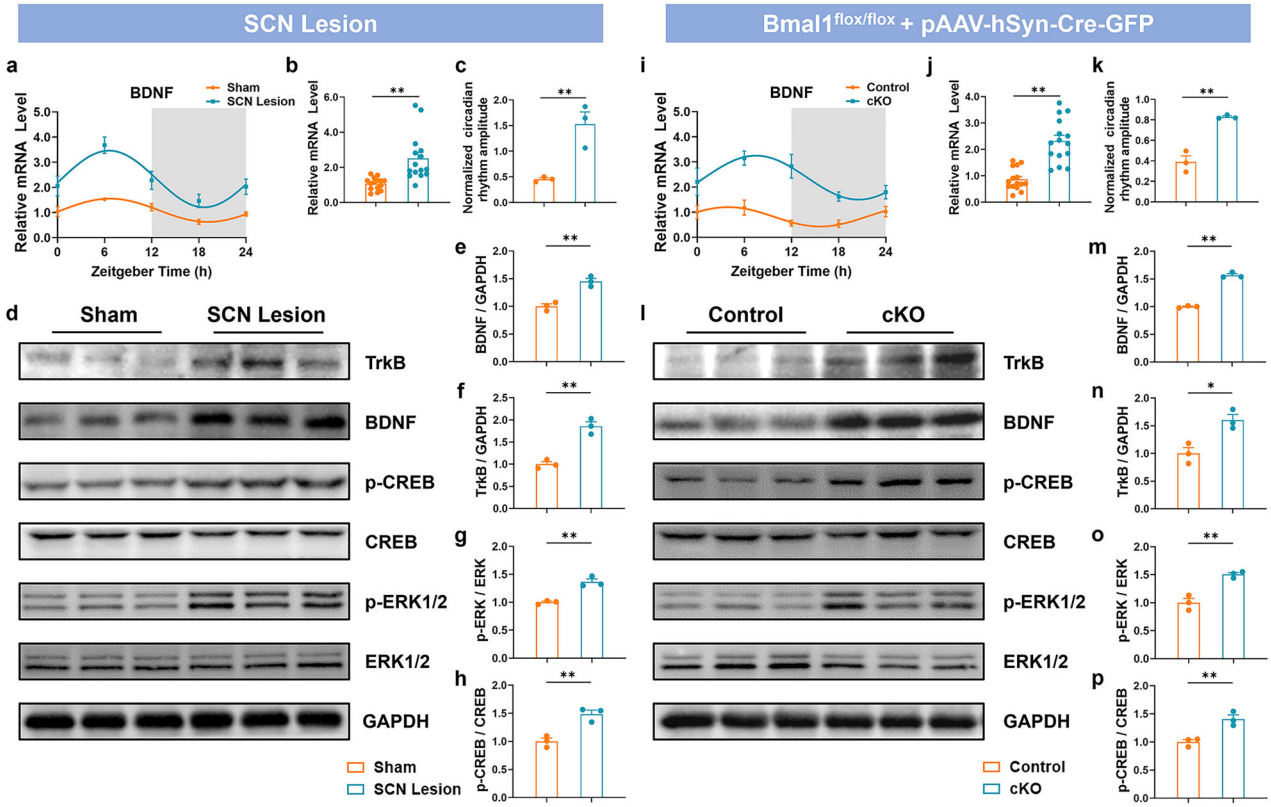

Fig. 4 Effect of bilateral SCN lesions and Conditional knockout of Bmal1 on BDNF-TrkB pathway upregulation in the striatum. a Cosine curve graph of relative BDNF mRNA level of Sham and SCN Lesion groups. **b** Relative mRNA level of BDNF. n = 15. **c** Normalized circadian rhythm amplitude. n = 3. **d–h** Representative immunoblots and quantitative analyses of BDNF, TrkB, p-CREB, CREB, p-ERK (Thr202/Tyr204) and ERK expression. n = 3. **i** Cosine curve graph of relative mRNA level of Control and cKO groups. **j** Relative mRNA level of BDNF. n = 15. **k** Normalized circadian rhythm amplitude. n = 3. **l–p** Representative immunoblots and quantitative analyses of BDNF, TrkB, p-CREB, CREB, p-ERK (Thr202/Tyr204) and ERK expression. n = 3. Data are expressed as mean ± SEM, ANOVA, $*p < 0.05$, $**p < 0.01$, by two-tailed unpaired Student's t test.

The SCN serves as the master clock for circadian rhythms, coordinating the synthesis of "circadian clock proteins" in various regions, maintaining internal cycles via neural connections and projections. Integrity of SCN is necessary for the production of typical circadian rhythms [34]. Previous studies have demonstrated that SCN damage (caused by trauma or surgery) eliminated the circadian cycles of eating, sleeping, and the loss of behavioral and core temperature rhythms in mammals [35–37]. Furthermore, optogenetic activation inhibited SCN amplitude, thus exacerbating anxiety-like symptoms [38]. In this study, bilateral SCN lesions decreased the amplitude of diurnal temperature oscillations and caused anxiety- and depression-like behaviors.

Further research is warranted to elucidate the pathogenic mechanisms underlying the impact of circadian rhythm disruption on mood. The SCN is a complex structure with multiple nerve projections extending to various regions of the brain. Moreover, these nerve projections receive inputs from several brain areas, establishing connections with crucial brain regions associated with emotional regulation [16]. In our study, using anterograde tracers, we found that SCN neurons projected into the striatum. The colocalization of c-Fos and eGFP fluorescence increased, indicating that the SCN-striatum neuronal connection was activated after SCN injury. Furthermore, SCN lesions disrupted the circadian rhythms of clock genes in the striatum. Specifically, the group with SCN lesions had significantly lower oscillation amplitudes of Bmal1 in the striatum compared to the sham group. Variations in circadian clock genes play a role in mood regulation. For instance, reducing Bmal1 expression in the SCN induced anxiety-like and depressive-like behaviors [13, 14]. The expression of Clock in the ventral tegmental area (VTA) modulated mood, anxiety, and locomotor behavior, and Clock knock down in the VTA aggravated depression-like behavior [39]. The expression oscillations of Cry2, Per1, and Per2 have been shown to be disrupted in a mouse model of depression, and deletion of Cry2 promoted depression-like behavior [15, 40, 41]. Furthermore, genetic factors influence the occurrence of neuropsychiatric disorders, including schizophrenia, bipolar disorder, and depression [2, 3, 5]. Clock, Per1, and Bmal1 mRNA levels were significantly increased in the morning in the peripheral blood leukocytes of people with a history of depression [42]. Together, these results highlighted the complex relationship among the SCN, striatum, and genetic diversity in circadian clock genes in influencing emotional well-being. Further research is necessary to elucidate the specific molecular and neural mechanisms driving these interactions and their significance for mood control. In our subsequent experiments, we aimed to explore the precise molecular mechanisms by which the SCN influences mood through its regulation of the striatum.

BDNF and its high-affinity receptor, TrkB, are abundantly dispersed throughout the central nervous system [43]. It is reported that BDNF exerts antidepressant and prodepressant effects in different brain regions [44]. The BDNF-TrkB pathway modulated mood and was influenced by circadian rhythms [45–47]. In this intricate process, the BDNF exhibited rhythmic expression patterns in the SCN and striatum. This signaling pathway may alter the sensitivity of the SCN pacemaker to light cues, thereby impacting mood regulation [48–51]. Additionally, the SCN regulated the circadian oscillation of the adenylyl cyclase/MAPK pathway [52]. The expression of the Cyclic AMP response element-binding protein (CREB) displayed an endogenously-controlled 24 h variation and its activation can promote depression-

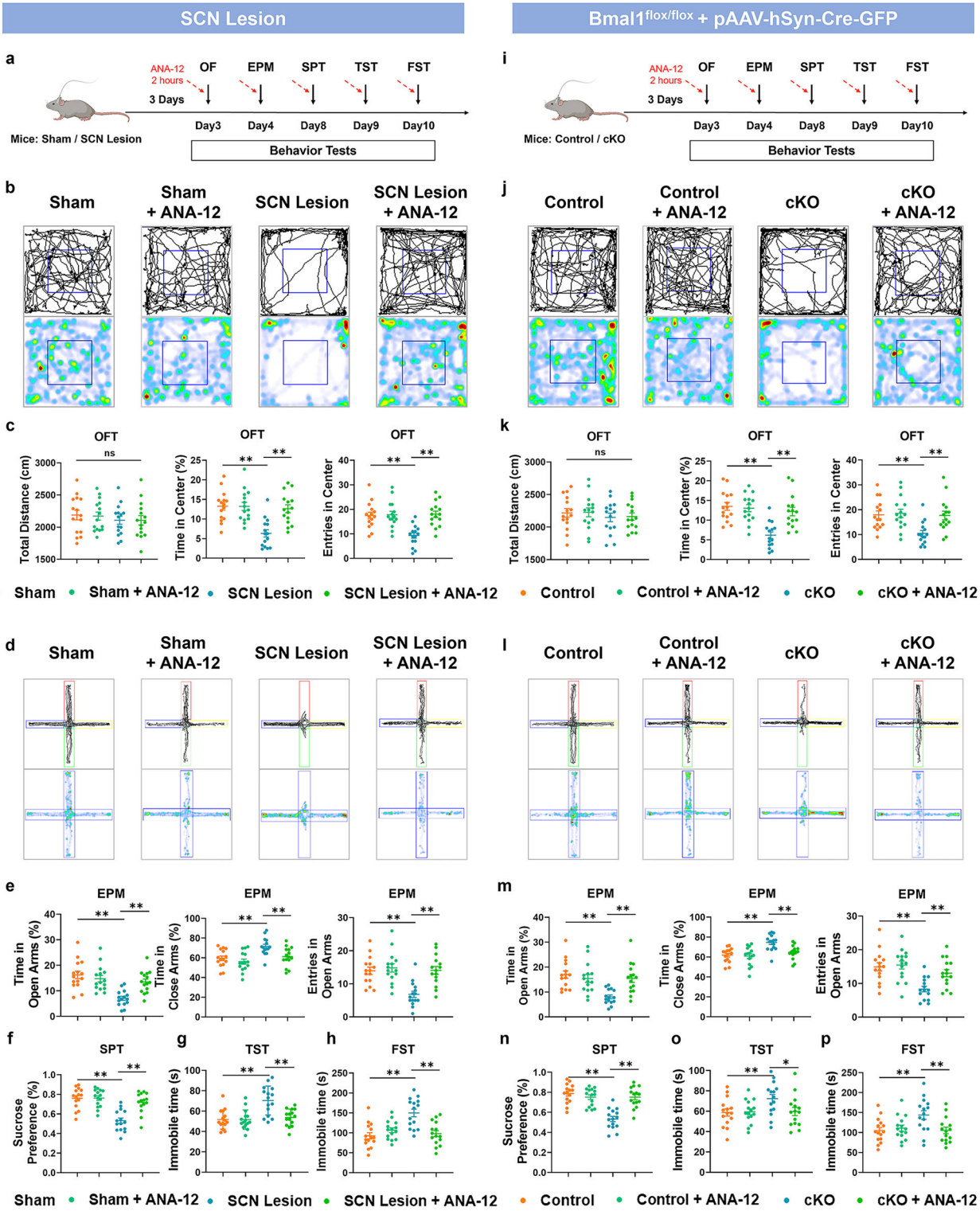

Fig. 5 ANA-12 ameliorated anxiety-like and depressive-like behaviors in SCN Lesion and cKO mice. a Experimental design. **b** Trajectory map of Sham, Sham + ANA-12, SCN Lesion, and SCN Lesion + ANA-12 groups in the OFT. **c** Total distance, center time percentage, and entries into center in the OFT. (n = 15, respectively). **d** Trajectory map of Sham, Sham + ANA-12, SCN Lesion, and SCN Lesion + ANA-12 groups in the EPM. **e** Open arms time percentage, entries into open arms, and close arms time percentage in the EPM (n = 15, respectively). **f** Sucrose preference percentage in the SPT (n = 15, respectively). **g** Immobility time in the TST (n = 15, respectively). **h** Immobility time in the FST (n = 15, respectively). **i** Experimental design. **j** Trajectory map of Control, Control + ANA-12, cKO, and cKO + ANA-12 groups in the OFT. **k** Total distance, center time percentage, and entries into center in the OFT. (n = 15, respectively). **l** Trajectory map of Control, cKO, and cKO + ANA-12 groups in the EPM. **m** Open arms time percentage, entries into open arms, and close arms time percentage in the EPM (n = 15, respectively). **n** Sucrose preference percentage in the SPT (n = 15, respectively). **o** Immobility time in the TST (n = 15, respectively). **p** Immobility time in the FST (n = 15, respectively). Data are expressed as mean ± SEM, ANOVA, $*p < 0.05$, $**p < 0.01$, by two-tailed unpaired Student's t test. OFT, open field test; EPM, elevated plus maze test; SPT, sucrose preference test; TST, tail suspension test; FST, forced swim test.

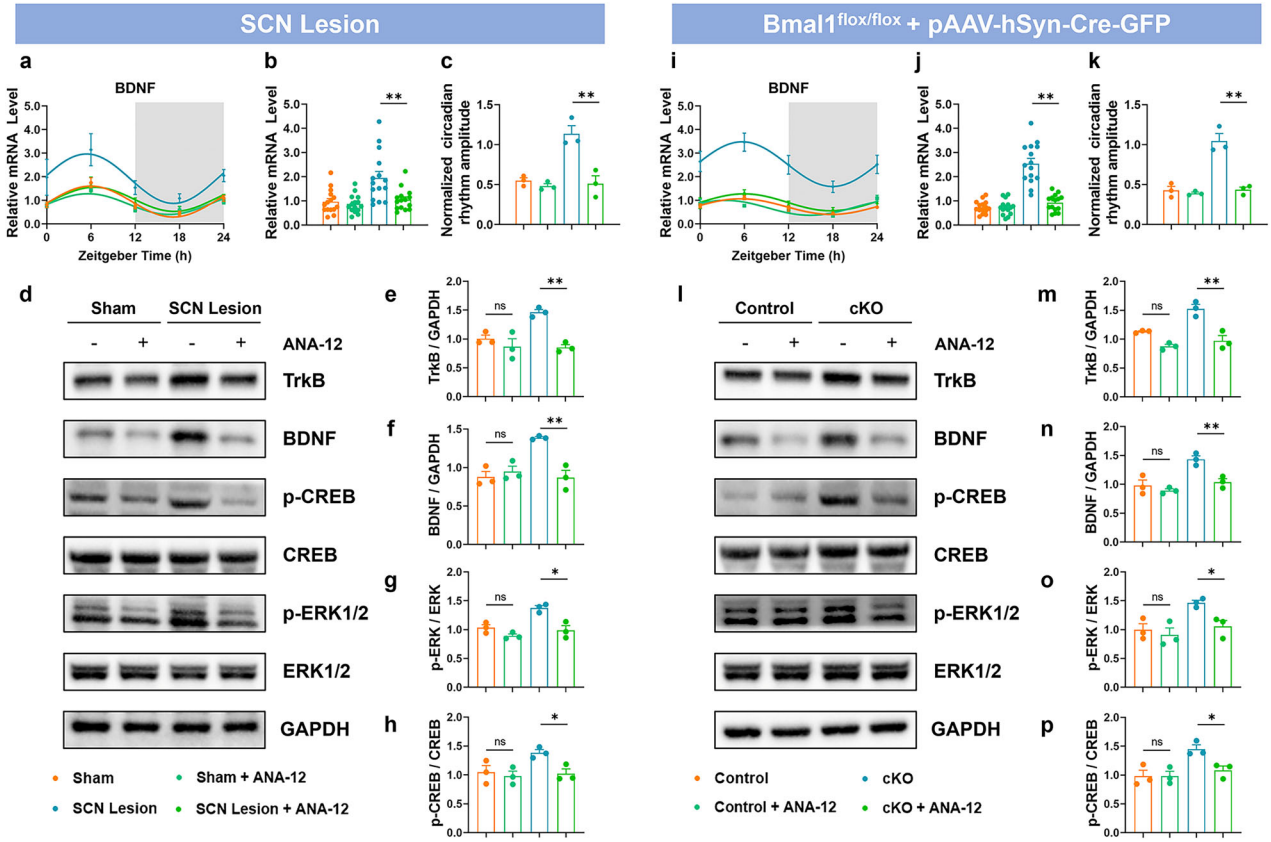

Fig. 6 ANA-12 downregulated BDNF-TrkB signaling in SCN Lesion and cKO mice. a Cosine curve graph of relative mRNA level of Sham, Sham + ANA-12, SCN Lesion, and SCN Lesion + ANA-12 groups. **b** Relative mRNA level of BDNF. n = 15. **c** Normalized circadian rhythm amplitude. n = 3. **d–h** Representative immunoblots and quantitative analyses of BDNF, TrkB, p-CREB, CREB, p-ERK (Thr202/Tyr204) and ERK expression. n = 3. **i** Cosine curve graph of relative mRNA level of Control, Control + ANA-12, cKO, and cKO + ANA-12 groups. **j** Relative mRNA level of BDNF. n = 15. **k** Normalized circadian rhythm amplitude. n = 3. **l–p** Representative immunoblots and quantitative analyses of BDNF, TrkB, p-CREB, CREB, p-ERK (Thr202/Tyr204) and ERK expression. n = 3. Data are expressed as mean ± SEM, ANOVA, $*p < 0.05$, $**p < 0.01$, by two-tailed unpaired Student's t test.

like behavior at the level of VTA-to-NAc circuit [18, 52, 53]. Elsewhere, it was found that continuous optogenetic phasic stimulation of the VTA-NAc circuit during chronic social defeat stress (CSDS) exacerbated depressive-like behaviors, and these symptoms were weakened by blocking the BDNF-TrkB pathway in the NAc [24]. As a result, we focused on the BDNF-TrkB pathway in the striatum. It was observed that the mRNA level of BDNF in striatum for the sham group displayed a circadian rhythm, with the levels increasing throughout the subjective night and decreasing during the subjective day. For the SCN lesion group, the striatum exhibited an increase in the mRNA level and oscillation amplitude of BDNF, demonstrating an inverse trend: high expression during the subjective day and low expression at night, with the peak value appearing during the subjective day (ZT6). Based on our research findings, we inferred that SCN regulates the circadian rhythm of BDNF in the striatum. Notably, the BDNF-TrkB pathway is activated, leading to the upregulation of phosphorylated CREB and ERK protein expression after SCN injury. To confirm the role of the BDNF-TrkB pathway, we utilized ANA-12 to downregulate this pathway in the striatum, successfully reversing anxiety- and depression-like behaviors in mice. This suggests that mood disorders linked to disruptions in circadian rhythm may potentially be mediated through this pathway.

Bmal1 is the only single-clock gene knockout in mice that alleviates all rhythmic behavioral activities, and participates in transcription–translation negative feedback loops (TIFF) [54]. Bmal1 has attracted significant attention in the field of mood disorders. About 70% of individuals grappling with depression and a notable 20–30% of those dealing with anxiety disorders concurrently experienced disturbances in their circadian rhythm, notably including symptoms like insomnia [55, 56]. In depressed rats, the amplitude of Bmal1 in the nucleus accumbens was decreased, but its overall expression increased [57]. Treatment with trazodone and citalopram in rats with MDD resulted in reduced expression of BDNF, Bmal1, and Per1 in the NAc of the striatum, ultimately leading to antidepressant effects [58]. Considering the role of Bmal1 in circadian rhythms, we postulate that Bmal1 regulates SCN function and modulates the rhythmic expression of striatal circadian clock proteins and BDNF via the SCN -striatum neural connection. Interestingly, this hypothesis was supported by the experimental findings. Mice with conditional Bmal1 knockout in SCN exhibited disruptions in core body temperature rhythm, as well as anxiety- and depression-like behaviors. In the SCN and striatum, the Bmal1 oscillations exhibited reduced amplitude, accompanied by changes in the amplitude of other clock proteins. Simultaneously, there was an increase in BDNF expression levels and oscillatory amplitudes in the striatum, accompanied by an upregulation of the BDNF-TrkB pathway. Our study introduces an innovative perspective, proposing that the potential linkage between the pathological mechanisms governing circadian rhythms and anxiety- and depression-like behaviors may be attributed to the regulation of SCN neuron Bmal1 and the striatal BDNF-TrkB pathway.

Limitations

One limitation of this study is the temporal scope of our observations, which were confined to a 24h period. Extending these observations

to 48 or 72 h might have yielded more robust insights into the dynamics of circadian rhythm gene expression. Additionally, while anatomical tracing was employed to establish the connectivity between the SCN and the striatum, the functional dynamics of these connections were not explored. Future studies incorporating optogenetic techniques would be instrumental in elucidating the functional implications of these anatomical pathways. Furthermore, precise mechanisms underlying the observed effects could be better elucidated by directly knocking down TrkB or BDNF in the striatum.

This study investigated the effects of circadian disruption in neural circuits on anxiety- and depression-like behaviors, using only male mice to eliminate the potential confounding influence of estrogen signaling on circadian regulation. While this approach simplifies the interpretation of our findings, it inherently limits their applicability to both sexes. Anxiety and depression are more prevalent in females [59], and estrogen signaling may influence circadian rhythms and mood regulation in sex-specific ways [60]. Future research should include female mice to evaluate potential sex differences in the effects of SCN disruptions on the BDNF-TrkB pathway. Addressing this limitation is crucial for advancing our understanding of the sex-specific mechanisms underlying circadian and mood-related processes.

DATA AVAILABILITY

All data needed to evaluate the conclusions in the paper are presented in the paper.

REFERENCES

1. Shen Y, Lv Q, Xie W, Gong S, Zhuang S, Liu J, et al. Circadian disruption and sleep disorders in neurodegeneration. Transl Neurodegener. 2023;12:8.
2. Dollish HK, Tsyglakova M, Mcclung CA. Circadian rhythms and mood disorders: time to see the light. Neuron. 2024;112:25–40.
3. Hickie IB, Crouse JJ. Sleep and circadian rhythm disturbances: plausible pathways to major mental disorders? World Psychiatry. 2024;23:150–1.
4. Lyall LM, Wyse CA, Graham N, Ferguson A, Lyall DM, Cullen B, et al. Association of disrupted circadian rhythmicity with mood disorders, subjective wellbeing, and cognitive function: a cross-sectional study of 91 105 participants from the UK biobank. Lancet Psychiatry. 2018;5:507–14.
5. Walker WN, Walton JC, Devries AC, Nelson RJ. Circadian rhythm disruption and mental health. Transl Psychiatry. 2020;10:28.
6. Russo SJ, Nestler EJ. The brain reward circuitry in mood disorders. Nat Rev Neurosci. 2013;14:609–25.
7. Asarnow LD, Soehner A, Dolsen E, Dong L, Harvey AG. Report from a randomized control trial: improved alignment between circadian biology and sleep-wake behavior as a mechanism of depression symptom improvement in evening-type adolescents with depressive symptoms. J Child Psychol Psychiatry. 2023;64:1652–64.
8. Sato S, Bunney B, Mendoza-Viveros L, Bunney W, Borrelli E, Sassone-Corsi P, et al. Rapid-acting antidepressants and the circadian clock. Neuropsychopharmacology. 2022;47:805–16.
9. Wirz-Justice A. Diurnal variation of depressive symptoms. Dialogues Clin Neurosci. 2008;10:337–43.
10. Blanken TF, Borsboom D, Penninx BW, Van Someren EJ. Network outcome analysis identifies difficulty initiating sleep as a primary target for prevention of depression: a 6-year prospective study. Sleep. 2020;43:zsz288.
11. Brown JP, Martin D, Nagaria Z, Verceles AC, Jobe SL, Wickwire EM. Mental health consequences of shift work: an updated review. Curr Psychiatry Rep. 2020;22:7.
12. Chen PJ, Huang CL, Weng SF, Wu MP, Ho CH, Wang JJ, et al. Relapse insomnia increases greater risk of anxiety and depression: evidence from a population-based 4-year cohort study. Sleep Med. 2017;38:122–9.
13. Landgraf D, Long JE, Proulx CD, Barandas R, Malinow R, Welsh DK. Genetic disruption of circadian rhythms in the suprachiasmatic nucleus causes helplessness, behavioral despair, and anxiety-like behavior in mice. Biol Psychiatry. 2016;80:827–35.
14. Qiu P, Jiang J, Liu Z, Cai Y, Huang T, Wang Y, et al. BMAL1 knockout macaque monkeys display reduced sleep and psychiatric disorders. Natl Sci Rev. 2019;6:87–100.
15. Savalli G, Diao W, Berger S, Ronovsky M, Partonen T, Pollak DD. Anhedonic behavior in cryptochrome 2-deficient mice is paralleled by altered diurnal patterns of amygdala gene expression. Amino Acids. 2015;47:1367–77.
16. Paul JR, Davis JA, Goode LK, Becker BK, Fusilier A, Meador-Woodruff A, et al. Circadian regulation of membrane physiology in neural oscillators throughout the brain. Eur J Neurosci. 2020;51:109–38.
17. Castro DC, Bruchas MR. A motivational and neuropeptidergic hub: anatomical and functional diversity within the nucleus accumbens shell. Neuron. 2019;102:529–52.
18. Nestler EJ, Carlezon WJ. The mesolimbic dopamine reward circuit in depression. Biol Psychiatry. 2006;59:1151–9.
19. Pasquereau B, Drui G, Saga Y, Richard A, Millot M, Metereau E, et al. Selective serotonin reuptake inhibitor treatment retunes emotional valence in primate ventral striatum. Neuropsychopharmacology. 2021;46:2073–82.
20. Wang W, Xie X, Zhuang X, Huang Y, Tan T, Gangal H, et al. Striatal mu-opioid receptor activation triggers direct-pathway GABAergic plasticity and induces negative affect. Cell Rep. 2023;42:112089.
21. Asadian N, Parsaie H, Vafaei AA, Dadkhah M, Omoumi S, Sedaghat K. Chronic light deprivation induces different effects on spatial and fear memory and hippocampal BDNF/TRKB expression during light and dark phases of rat diurnal rhythm. Behav Brain Res. 2022;418:113638.
22. Castren E, Monteggia LM. Brain-derived neurotrophic factor signaling in depression and antidepressant action. Biol Psychiatry. 2021;90:128–36.
23. Li W, Ali T, Zheng C, He K, Liu Z, Shah FA, et al. Anti-depressive-like behaviors of APN KO mice involve trkb/BDNF signaling related neuroinflammatory changes. Mol Psychiatry. 2022;27:1047–58.
24. Wook KJ, Labonte B, Engmann O, Calipari ES, Juarez B, Lorsch Z, et al. Essential role of mesolimbic brain-derived neurotrophic factor in chronic social stress-induced depressive behaviors. Biol Psychiatry. 2016;80:469–78.
25. Miyanishi H, Muramatsu SI, Nitta A. Striatal shati/nat8l-BDNF pathways determine the sensitivity to social defeat stress in mice through epigenetic regulation. Neuropsychopharmacology. 2021;46:1594–605.
26. Walsh JJ, Friedman AK, Sun H, Heller EA, Ku SM, Juarez B, et al. Stress and CRF gate neural activation of BDNF in the mesolimbic reward pathway. Nat Neurosci. 2014;17:27–9.
27. Leng L, Zhuang K, Liu Z, Huang C, Gao Y, Chen G, et al. Menin deficiency leads to depressive-like behaviors in mice by modulating astrocyte-mediated neuroinflammation. Neuron. 2018;100:551–63.
28. Liang X, Liang X, Zhao Y, Ding Y, Zhu X, Zhou J, et al. Dysregulation of the suprachiasmatic nucleus disturbs the circadian rhythm and aggravates epileptic seizures by inducing hippocampal GABAergic dysfunction in c57BL/6 mice. J Pineal Res. 2024;76:e12993.
29. Liang XS, Qian TL, Xiong YF, Liang XT, Ding YW, Zhu XY, et al. IRAK-m ablation promotes status epilepticus-induced neuroinflammation via activating m1 microglia and impairing excitatory synaptic function. Mol Neurobiol. 2023;60:5199–213.
30. Krishnan V, Han MH, Graham DL, Berton O, Renthal W, Russo SJ, et al. Molecular adaptations underlying susceptibility and resistance to social defeat in brain reward regions. Cell. 2007;131:391–404.
31. Adachi M, Autry AE, Mahgoub M, Suzuki K, Monteggia LM. TrkB signaling in dorsal raphe nucleus is essential for antidepressant efficacy and normal aggression behavior. Neuropsychopharmacology. 2017;42:886–94.
32. Cazorla M, Premont J, Mann A, Girard N, Kellendonk C, Rognan D. Identification of a low-molecular weight TrkB antagonist with anxiolytic and antidepressant activity in mice. J Clin Invest. 2011;121:1846–57.
33. Patke A, Young MW, Axelrod S. Molecular mechanisms and physiological importance of circadian rhythms. Nat Rev Mol Cell Biol. 2020;21:67–84.
34. Blancas-Velazquez AS, Bering T, Bille S, Rath MF. Role and neural regulation of clock genes in the rat pineal gland: clock modulates amplitude of rhythmic expression of aanat encoding the melatonin-producing enzyme. J Pineal Res. 2023;75:e12893.
35. Edgar DM, Dement WC, Fuller CA. Effect of SCN lesions on sleep in squirrel monkeys: evidence for opponent processes in sleep-wake regulation. J Neurosci. 1993;13:1065–79.
36. Liu S, Chen XM, Yoda T, Nagashima K, Fukuda Y, Kanosue K. Involvement of the suprachiasmatic nucleus in body temperature modulation by food deprivation in rats. Brain Res. 2002;929:26–36.
37. Purnell BS, Buchanan GF. Free-running circadian breathing rhythms are eliminated by suprachiasmatic nucleus lesion. J Appl Physiol (1985). 2020;129:49–57.
38. Vadnie CA, Petersen KA, Eberhardt LA, Hildebrand MA, Cerwensky AJ, Zhang H, et al. The suprachiasmatic nucleus regulates anxiety-like behavior in mice. Front Neurosci. 2021;15:765850.
39. Mukherjee S, Coque L, Cao J, Kumar J, Chakravarty S, Asaithamby A, et al. Knockdown of clock in the ventral tegmental area through RNA interference results in a mixed state of mania and depression-like behavior. Biol Psychiatry. 2010;68:503–11.
40. Porcu A, Vaughan M, Nilsson A, Arimoto N, Lamia K, Welsh DK. Vulnerability to helpless behavior is regulated by the circadian clock component CRYPTOCHROME in the mouse nucleus accumbens. Proc Natl Acad Sci USA. 2020;117:13771–82.
41. Savalli G, Diao W, Schulz S, Todtova K, Pollak DD. Diurnal oscillation of amygdala clock gene expression and loss of synchrony in a mouse model of depression. Int J Neuropsychopharmacol. 2015;18:1–11.

42. Gouin JP, Connors J, Kiecolt-Glaser JK, Glaser R, Malarkey WB, Atkinson C, et al. Altered expression of circadian rhythm genes among individuals with a history of depression. J Affect Disord. 2010;126:161–6.
43. Notaras M, van den Buuse M. Neurobiology of BDNF in fear memory, sensitivity to stress, and stress-related disorders. Mol Psychiatry. 2020;25:2251–74.
44. Lei T, Dong D, Song M, Sun Y, Liu X, Zhao H. Rislenemdaz treatment in the lateral habenula improves despair-like behavior in mice. Neuropsychopharmacology. 2020;45:1717–24.
45. Guan Y, Xu M, Zhang Z, Liu C, Zhou J, Lin F, et al. Maternal circadian disruption before pregnancy impairs the ovarian function of female offspring in mice. Sci Total Environ. 2023;864:161161.
46. Liang FQ, Sohrabji F, Miranda R, Earnest B, Earnest D. Expression of brain-derived neurotrophic factor and its cognate receptor, TrkB, in the rat suprachiasmatic nucleus. Exp Neurol. 1998;151:184–93.
47. Luan J, Zhang S, Xu Y, Wen L, Feng X. Effects of microplastic exposure on the early developmental period and circadian rhythm of zebrafish (danio rerio): a comparative study of polylactic acid and polyglycolic acid. Ecotoxicol Environ Saf. 2023;258:114994.
48. Buniyaadi A, Prabhat A, Bhardwaj SK, Kumar V. Night melatonin levels affect cognition in diurnal animals: molecular insights from a corvid exposed to an illuminated night environment. Environ Pollut. 2022;308:119618.
49. Girardet C, Lebrun B, Cabirol-Pol MJ, Tardivel C, Francois-Bellan AM, Becquet D, et al. Brain-derived neurotrophic factor/TrkB signaling regulates daily astroglial plasticity in the suprachiasmatic nucleus: electron-microscopic evidence in mouse. Glia. 2013;61:1172–7.
50. Meltser I, Cederroth CR, Basinou V, Savelyev S, Lundkvist GS, Canlon B. TrkB-mediated protection against circadian sensitivity to noise trauma in the murine cochlea. Curr Biol. 2014;24:658–63.
51. Walker WN, Borniger JC, Gaudier-Diaz MM, Hecmarie MO, Pascoe JL, Courtney DA, et al. Acute exposure to low-level light at night is sufficient to induce neurological changes and depressive-like behavior. Mol Psychiatry. 2020;25:1080–93.
52. Phan TX, Chan GC, Sindreu CB, Eckel-Mahan KL, Storm DR. The diurnal oscillation of MAP (mitogen-activated protein) kinase and adenylyl cyclase activities in the hippocampus depends on the suprachiasmatic nucleus. J Neurosci. 2011;31:10640–7.
53. Autry AE, Monteggia LM. Brain-derived neurotrophic factor and neuropsychiatric disorders. Pharmacol Rev. 2012;64:238–58.
54. Bunger MK, Wilsbacher LD, Moran SM, Clendenin C, Radcliffe LA, Hogenesch JB, et al. Mop3 is an essential component of the master circadian pacemaker in mammals. Cell. 2000;103:1009–17.
55. Geoffroy PA, Hoertel N, Etain B, Bellivier F, Delorme R, Limosin F, et al. Insomnia and hypersomnia in major depressive episode: prevalence, sociodemographic characteristics and psychiatric comorbidity in a population-based study. J Affect Disord. 2018;226:132–41.
56. Ohayon MM. Observation of the natural evolution of insomnia in the american general population cohort. Sleep Med Clin. 2009;4:87–92.
57. Christiansen SL, Bouzinova EV, Fahrenkrug J, Wiborg O. Altered expression pattern of clock genes in a rat model of depression. Int J Neuropsychopharmacol. 2016;19:pyw061.
58. Carboni L, Rullo L, Caputi FF, Stamatakos S, Candeletti S, Romualdi P. Chronic trazodone and citalopram treatments increase trophic factor and circadian rhythm gene expression in rat brain regions relevant for antidepressant efficacy. Int J Mol Sci. 2022;23:14041.
59. Vos T, Lim SS, Abbafati C, Abbas KM, Abbasi M, Abbasifard M, et al. Global burden of 369 diseases and injuries in 204 countries and territories, 1990–2019: a systematic analysis for the global burden of disease study 2019. The Lancet. 2020;396:1204–22.
60. Bailey M, Silver R. Sex differences in circadian timing systems: implications for disease. Front Neuroendocrinol. 2014;35:111–39.

ACKNOWLEDGEMENTS

We thank Prof. Hai-Tao Wang (Department of Neuropharmacology and Drug Discovery, School of Pharmaceutical Sciences, Southern Medical University) and Dr. Hui-Jie Mi (Academy for Advanced Interdisciplinary Studies, Peking University) for their insightful recommendations. We also sincerely thank the editor and anonymous reviewers for their constructive feedback.

AUTHOR CONTRIBUTIONS

Xiaotao Liang performed the biochemical experiments and Immunofluorescence staining and wrote the first draft of the manuscript. Xiaotao Liang, Xiaoyu Zhu, and Jing Qiu completed virus injection, animal behavior, and behavioral analysis. Yuewen Ding assisted with Gene Expression Omnibus (GEO) database analysis. Yifan Xiong and Xiaoqin Shen performed data analysis. Yuewen Ding, Jieli Zhou discussed the manuscripts. Xiaoshan Liang and Wei Xie designed the study, wrote the paper, and supervised all aspects of the project.

FUNDING

This work was supported by National Natural Science Foundation of China (No. 82074265, 82405378); Natural Science Foundation of Guangdong Province, China (No. 2021A1515011505); China Postdoctoral Science Foundation (No. 2024M761351); Construction Fund of Key Disciplines of Traditional Chinese Medicine in Guangdong, China (No. 20220105); The second national famous Traditional Chinese Medicine Inheritance Studio (No. G724290126).

COMPETING INTERESTS

The authors report no biomedical financial interests or potential conflicts of interest.

ADDITIONAL INFORMATION

Supplementary information The online version contains supplementary material available at https://doi.org/10.1038/s41398-025-03313-7.

Correspondence and requests for materials should be addressed to Xiaoshan Liang or Wei Xie.